Investigation of the evolution of single domain (111)B CdTe films by molecular beam epitaxy on miscut (001)Si substrate

Y. Xin,[a] N. D. Browning, S. Rujirawat, S. Sivananthan, and Y. P. Chen
Department of Physics, University of Illinois at Chicago, Chicago, Ilinois 60607-7059

P. D. Nellist
Cavendish Laboratory, Cambridge University, Madingley Road, Cambridge CB3 0HE, United Kingdom

S. J. Pennycook
Solid State Division, Oak Ridge National Laboratory, Oak Ridge, Tennessee 37831-6031

(Received 15 May 1998; accepted for publication 22 July 1998)

A comprehensive view of the microstructure of (111)B CdTe films grown on miscut (001)Si substrates by molecular beam epitaxy has been obtained by transmission electron microscopy and scanning transmission electron microscopy. It is found that in the initial growth stage, CdTe nucleates with a dominance of one particular domain: a domain with (111)B polarity and orientation of [11−2]CdTe//[1−10]Si, although there are also some other domains of different polarity and orientation. The dominance of one type domain is due to the reduction of the surface symmetry by using the miscut substrate and by using optimum growth conditions. As the growth proceeds, a single-crystal film is produced by the dominating domain overgrowing the minority domains nucleated at the film–substrate interface. This results in the final film of single-crystal character having (111)B polarity with [11−2]CdTe along [1−10]Si. © *1998 American Institute of Physics.* [S0021-8979(98)09220-2]

I. INTRODUCTION

The direct band gap and capability for band-gap engineering make $Hg_{1-x}Cd_xTe$ (MCT) an ideal material for a wide range of applications, such as infrared detectors, large array x-ray or γ-ray detectors, and other optoelectronics. However, its physical properties make it difficult to grow high-quality material and fabricate devices. Although some of these difficulties can be overcome by the use of CdTe as a substrate for the epitaxial growth of MCT, applications are limited by its brittleness and expense. Recently, progress has been made by using a thin CdTe layer deposited on Si as an alternative substrate. There are many advantages of CdTe/Si as a substrate for the subsequent growth of MCT, i.e., Si provides inexpensive large buffer areas and strong support, and also the mature Si technology can facilitate monolithic integrated infrared focal plane array technology. Hence there has been continuous interest in the growth of CdTe on Si substrates.

Various growth methods, such as molecular beam epitaxy (MBE), metalorganic chemical vapor deposition (MOCVD),[1,2] metalorganic vapor phase epitaxy (MOVPE),[3] and hot wall epitaxy[4,5] have been used to grow CdTe films on Si substrates. For all techniques, problems arise from the large lattice mismatch of 19.3% between CdTe and Si. By adopting a specific orientation relationship between the CdTe epilayer and the (001)Si substrate, i.e., [111]CdTe//[001]Si, [1−10]CdTe//[110]Si, and [11−2]CdTe//[1−10]Si, the mismatch can be reduced to 3.4% along the [11−2]CdTe direction. However, although the mismatch is reduced, the fourfold symmetry of the (001)Si surface leads to multidomain growth, i.e., [11−2]CdTe could align parallel to either of the four ⟨110⟩ directions on the (001)Si surface. It has been shown that pretreatment of the substrate before growth and subsequent annealing, the use of an optimized VI/II ratio and a two-step growth process are important to obtain single-crystal films. In fact, by optimizing these growth parameters, and by using miscut (001)Si to reduce the symmetry of (001)Si surface arrangement, single-crystal (111)CdTe films are now routinely grown by MBE.[6–11] The best quality films attained so far have a double-crystal rocking curve full width at half maximum (DCRC FWHM) of 60 arcsec at a film thickness of 17 μm.

The focus of the present work is to investigate these high-quality single domain CdTe films on the miscut (001)Si substrates by utilizing transmission electron microscopy (TEM) and scanning transmission electron microscopy (STEM). By studying both thin (~50 nm) and thick (~5 μm) films, a comprehensive view of the evolution of the film after the initial nucleation stage is attained.

II. EXPERIMENT

In order to have a comprehensive view of the growth evolution of (111)CdTe on a (001)Si substrate, two types of samples are studied. The first has a CdTe layer thickness of 50 nm, thus allowing study of the initial growth stage, while the second type of sample, with a thickness of 4.8 μm, allows the final microstructure of the epitaxial film to be determined. The substrate used in both cases is a misoriented (001)Si wafer with tilt parameters $\theta=4°$, $\phi=28°$, where θ is the angle between Si[001] and the substrate surface normal,

[a]Also at Solid State Division, Oak Ridge National Laboratory, Oak Ridge, TN 37831-6031.

 © 1998 American Institute of Physics

Downloaded 04 Jun 2004 to 160.91.48.238. Redistribution subject to AIP license or copyright, see http://jap.aip.org/jap/copyright.jsp

and ϕ is the azimuthal angle with respect to [110]Si. All the Si substrates were cleaned before growth which was carried out in a Riber Opus45 MBE system as described in other papers.[11] The pretreatment of the substrate is identical for all films studied in this article, with an As or Te flux. Briefly, thin films were grown at 250 °C for 10 min with one cycle of annealing, while the thick films were grown at 250 °C for 10 min with subsequent growth at 310 °C for several hours at 0.7 μm growth rate including seven annealing cycles.

Various TEM and STEM imaging techniques are used for microscopic investigation including conventional diffraction contrast imaging techniques, such as bright field (BF), dark field (DF), weak beam DF, and convergent beam electron diffraction (CBED), and also the technique of high-resolution *Z*-contrast imaging. TEM/STEM samples were made in cross section and plan view by conventional procedures. Conventional TEM work was performed on Philips CM30 and CM20 microscopes, while *Z*-contrast imaging was done on a VG HB603 STEM operating at 300 kV with a resolution of 0.13 nm. *Z*-contrast microscopy differs significantly from conventional high-resolution imaging in the mechanism of image formation. By detecting electrons scattered at high angles, an incoherent image is obtained in which individual atomic columns have a brightness proportional to their mean square atomic number (Z). There are no contrast reversals in an incoherent image so that *Z*-contrast imaging provides direct compositional information at the atomic scale. When used in conjunction with conventional TEM techniques, this correlated approach to materials characterization provides unparalleled insight into the microstructure of the materials system.

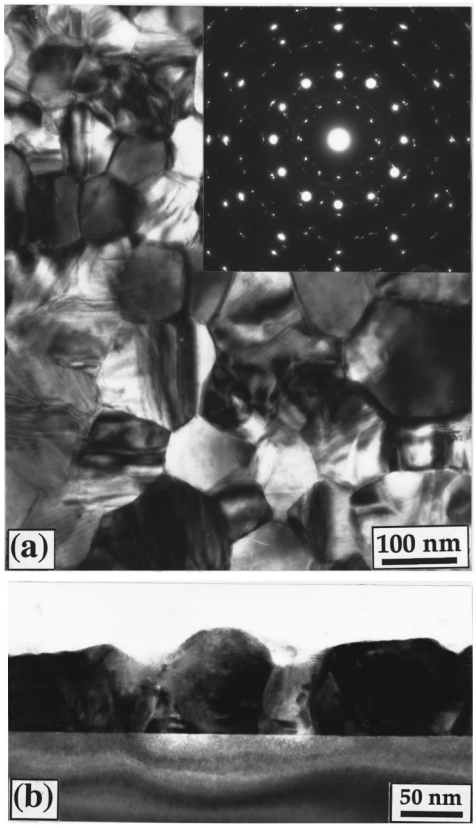

FIG. 1. (a) Plan-view bright field image down [111]CdTe/[001]Si of a thin film showing there are many grains at the nucleation stage; The inserted [111] selected area diffraction pattern showing that there are 90° rotated domains. (b) Cross-sectional view of the thin film down [110]Si, showing the side view of the grains above the CdTe/Si interface.

III. RESULTS

A. Microstructure of the thin films

To comprehend the initial growth process of the thick films, growth was halted after the initial stage and the microstructure examined. Both the plan view BF TEM image down [111]CdTe/[001]Si [Fig. 1(a)] and the cross-sectional image down [1−10]CdTe/[110]Si [Fig. 1(b)] show clearly that the CdTe layer is comprised of many small grains, with a lateral size ranging from ~0.5 μm to less than 0.1 μm. From the selected area diffraction pattern (inserted), it is seen that these are 90° rotated domains around the [111] axis. In order to determine the distribution of these domains, the weak beam DF images were taken of the plan view sample, shown in Figs. 2(a) and 2(b). In Fig. 2(a) the image is formed using the (2−20)CdTe diffraction spot from one of the domains, which is parallel to (220) Si. Here, domains with [11−2]CdTe//[1−10]Si have bright contrast. In Fig. 2(b), the (2−20)CdTe reflection parallel to (2−20)Si is used to image domains rotated by 90°. Comparing the two images, it is clearly seen that one type of domain dominates, being larger in size and interconnecting with other similar domains. The 90° rotated domains are smaller in size, isolated from each other, and surrounded by grains with the dominant orientation. From the arrangement of these domains the step morphology on the miscut (001)Si surface can be seen; the two types of domains are alternately aligned along [110]Si.

A sphalerite semiconductor like CdTe has two types of (111) surfaces, those terminating with triple-bonded Cd atoms denoted as (111)A surfaces, and those terminating with triple-bonded Te atoms, (111)B surfaces. For the growth of (111)CdTe on Si, CdTe domains could be grown with a (111)B polarity or (111)A polarity depending on growth conditions.[12,13] Many methods have been used to determine the polarity of CdTe crystals, e.g., x-ray scattering combined with chemical etching, channeling, or electron diffraction. In the case of multidomain thin films studied here, because of the small size of the domains and the presence of significant strain, among the possible TEM techniques suitable to study individual grains, high-resolution *Z*-contrast imaging is the most effective and intuitive method to ascertain polarity. As Te atoms have a higher atomic number than Cd atoms, Te columns are imaged brighter than Cd columns, and the polarity of the domain is directly determined without the need for any image simulations.

Figure 3(a) shows a *Z*-contrast image of one small CdTe domain looking down the [1−10]CdTe direction of a cross-sectional sample. At high magnification [Fig. 3(b)], the individual Te or Cd columns are clearly seen. By taking an intensity profile across one row of columns [Fig. 3(c)], it is obvious that the intensity is higher for the columns on the right. Relating this to the orientation of the Si substrate, it is therefore determined that this CdTe domain has B polarity,

Downloaded 04 Jun 2004 to 160.91.48.238. Redistribution subject to AIP license or copyright, see http://jap.aip.org/jap/copyright.jsp

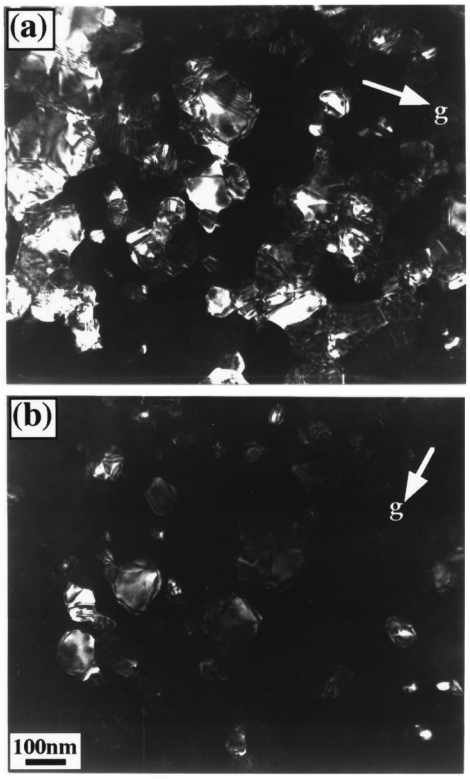

FIG. 2. Plan-view weak beam dark field images down [111]CdTe/[001]Si showing the distribution of the 90° rotated domains; (a) **g**=(2−20)CdTe//(220)Si; (b) **g**=(2−20)CdTe//(2−20)Si.

i.e., it is a domain with (111)B//(001)Si. Figure 4 shows another small CdTe domain from the same cross-sectional sample. It is obvious here that Cd atoms with weaker contrast are the terminating layer, and therefore this domain has A polarity, i.e., (111)A CdTe//(001)Si. It is interesting to note that in these thin films the majority of domains have (111)B polarity with a Te terminated layer, while only a small number of domains with opposite (111)A polarity are found to exist at the initial growth stage.

The main defects seen in the individual CdTe domains in this initial growth stage are stacking faults and microtwins. Shown in Fig. 5 are high resolution *Z*-contrast images of CdTe domains looking down [1−10]. Figure 5(a) shows a CdTe lattice image of a (111) twin at high magnification. From the intensity of the atomic columns, it is clearly seen that the polarity continues across the twin plane, as indicated by arrows. Figure 5(b) shows a CdTe domain with microtwins grown on both (111)A and (11−1)B planes. It is well known that due to the polarity of CdTe crystals, the (111)B surface (Te terminated surface) has a different growth rate from that of the (111)A surface (Cd-terminated surface).[14,15] This results in an anisotropic distribution of microtwins in CdTe crystals.[16–18] However, it is seen here that twinning can occur on both polar planes in the early growth stage when the growth has not reached its equilibrium state. It will be seen later that twinning occurs only on the (111)B plane at later stages of growth in thick films.

In summary, the general feature of this nucleation stage in the film growth is that it is very defective. Many small grains of different types of domains are nucleated at the substrate surface, but one orientation is dominant. The majority of the grains have (111)B polarity, but small number of the grains are (111)A orientated. The dominating domain has [11−2]CdTe//[1−10]Si with a (111)B polarity.

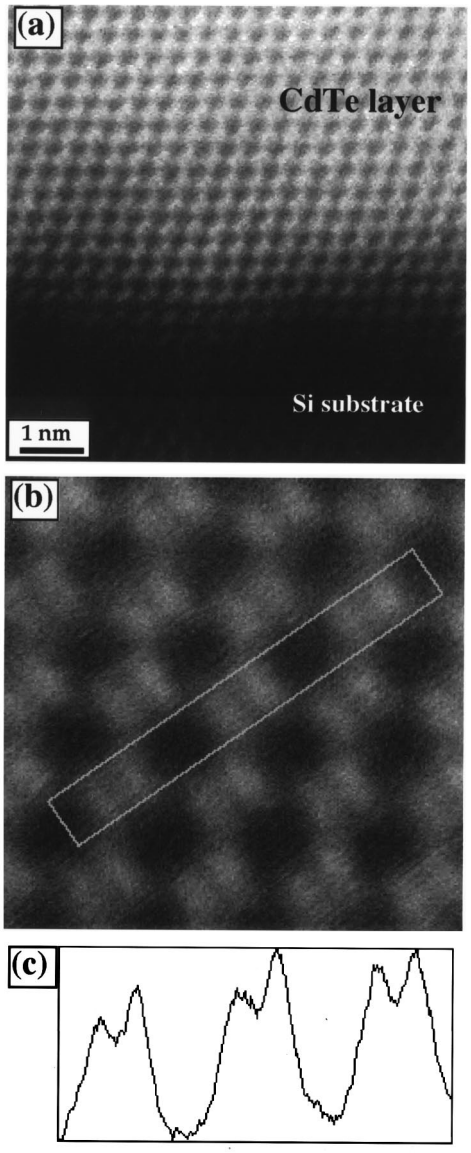

FIG. 3. (a) High-resolution *Z*-contrast image of a small (111)B domain above the CdTe/Si interface of a cross-sectional thin film, looking down [1−10]CdTe/[110]Si; (b) higher magnification of the CdTe layer of (a) showing the individual Cd and Te atomic columns; (c) Profile of the boxed region in (b) showing higher intensity of the terminating columns.

B. Microstructure of the thick films

Having examined the microstructure of the multidomain thin films, the single-crystal thick films are now discussed. Figure 6 shows BF and DF images of a cross-sectional sample of the thick film looking down [1−10]CdTe. Figure 6(a) is a BF image showing that the whole film is a single crystal, and there are densely populated lamellae twins confined to a region of 1.7 μm above the CdTe/Si interface, with the dislocations threading up in the film. A weak beam DF image of the same region [Fig. 6(b)] is formed using one (11−1) diffraction spot and showing only the threading dis-

Downloaded 04 Jun 2004 to 160.91.48.238. Redistribution subject to AIP license or copyright, see http://jap.aip.org/jap/copyright.jsp

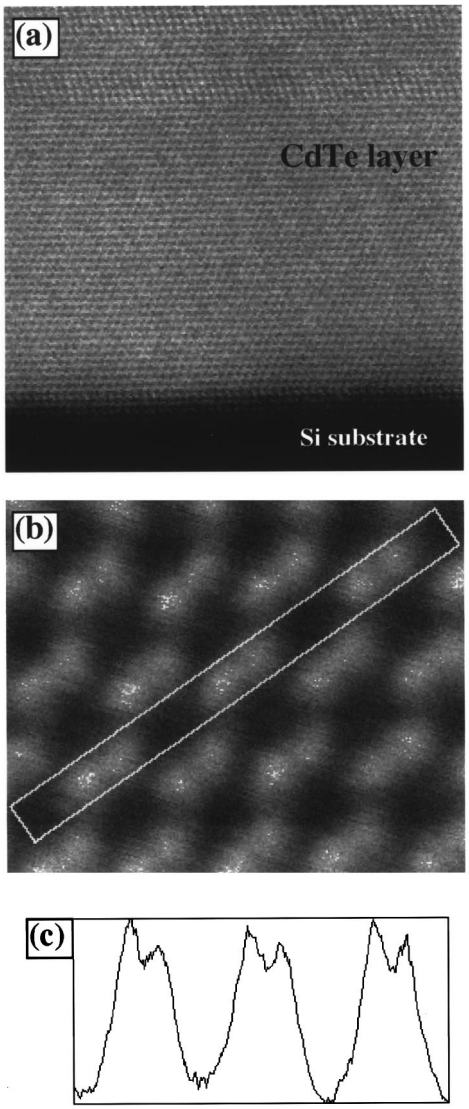

FIG. 4. (a) Lower magnification of a high-resolution *Z*-contrast image of a small (111)A domain above the CdTe/Si interface of a cross-sectional thin film looking down [1−10]CdTe/[110]Si; (b) higher magnification of the CdTe layer of (a) showing the individual Cd and Te atomic columns; (c) profile of the boxed region in (b) showing lower intensity of the terminating columns.

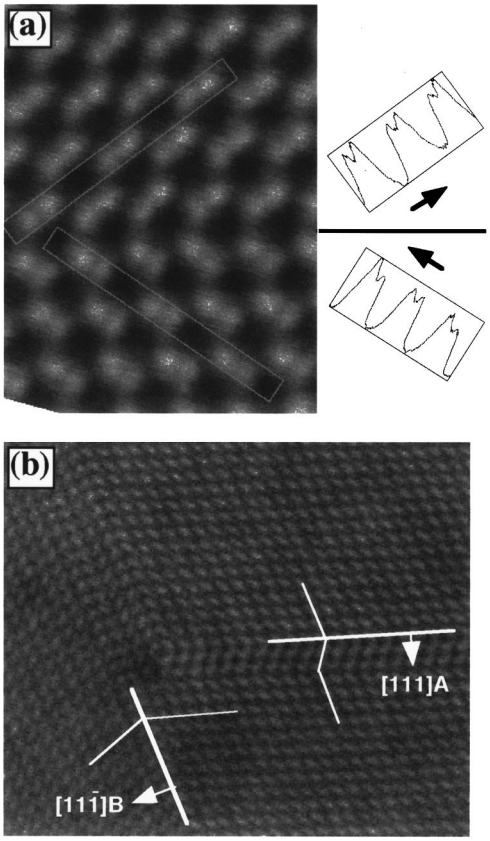

FIG. 5. (a) High-resolution *Z*-contrast image down [1−10] of a (111) twin in the CdTe layer, showing the polarity continuity across the twinning plane. (b) High-resolution *Z*-contrast image down [1−10] of another region of a CdTe layer of a thin film, showing the microtwins on both (11−1)B and (111)A planes.

locations. By comparison with Fig. 6(a), it is noticed that the threading dislocations originate from the disordered domain boundaries. The threading dislocations can be seen starting from the two grain boundaries, as well as from the boundaries at the overgrown small domains at the interface. The region just above the interface shows some contrast indicating the multidomain region, the same as the thin film mentioned earlier. It is clearly seen here that one source of threading dislocations generated in the films is from the disordered grain boundaries.

We now present several observations that show how a single domain film is obtained through this growth process. Figure 7 is a STEM annular dark field image of a cross-sectional view of the thick film sample down [1−10]CdTe. In the low magnification image [Fig. 7(a)], one small domain is seen embedded in the film matrix. An enlargement of the boxed region of Fig. 7(a) is given in Fig. 7(b), and clearly shows that the 90° rotated small domain, with an orientation of [11−2]CdTe, has been overgrown by the [1−10] matrix. Figure 7(c) is another high-resolution *Z*-contrast image showing twinning on the (111) plane from one of the 180° rotated domains that also results in the formation of a single domain from the two domains.

Due to the different properties of the two polar (111) surfaces, it is very important to know the terminating surface of the thick film. This is crucial if the film is to be used as a buffer layer to grow MCT. There has been much work on the determination of CdTe single crystal polarity since 1961.[19] Only in the eighties did a consensus begin to emerge that (111)B CdTe was the most suitable for epitaxial growth of MCT. Because the polarity of the films studied here was not determined from direct experimental data previously,[8,20] it is necessary to re-address this problem and determine the film polarity absolutely. Here, three methods are used to determine the polarity of the thick films; high-resolution *Z*-contrast imaging, CBED, and chemical etching. High-resolution *Z*-contrast imaging is the most direct method and does not involve reference samples. Figure 8 is a high-resolution *Z*-contrast image taken from a region close to the growth surface of a thick film looking down [1−10]. (The image is arranged in the way indicated.) Although the image is a little noisy due to contamination on the specimen surface, it is obvious from the image that atomic columns are

Downloaded 04 Jun 2004 to 160.91.48.238. Redistribution subject to AIP license or copyright, see http://jap.aip.org/jap/copyright.jsp

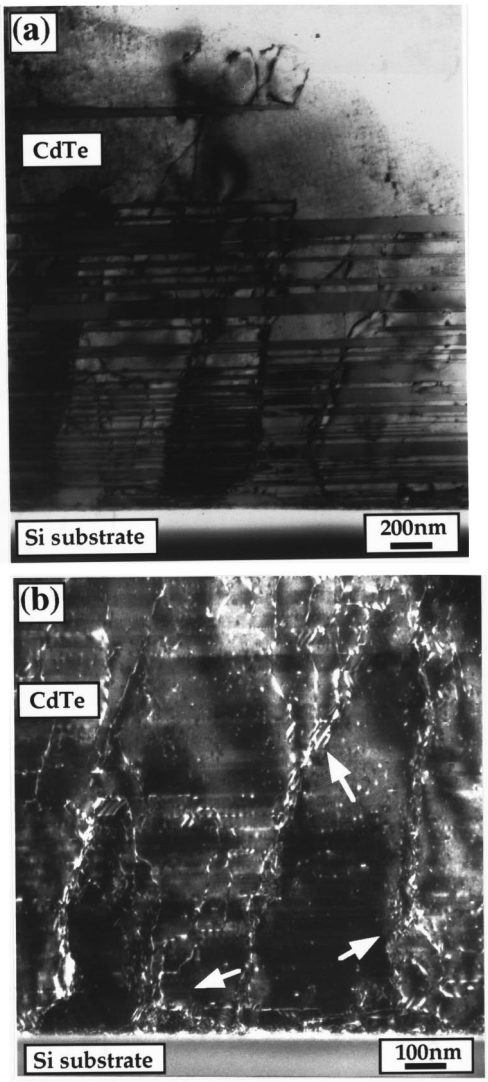

FIG. 6. (a) TEM bright field image of a cross-sectional view of a thick film down [1−10]CdTe/[110]Si showing the lamellae twins confined to the region above the CdTe/Si interface. (b) Weak beam dark field image of the same region as (a) showing only the threading dislocations, $\mathbf{g}=(11-1)$.

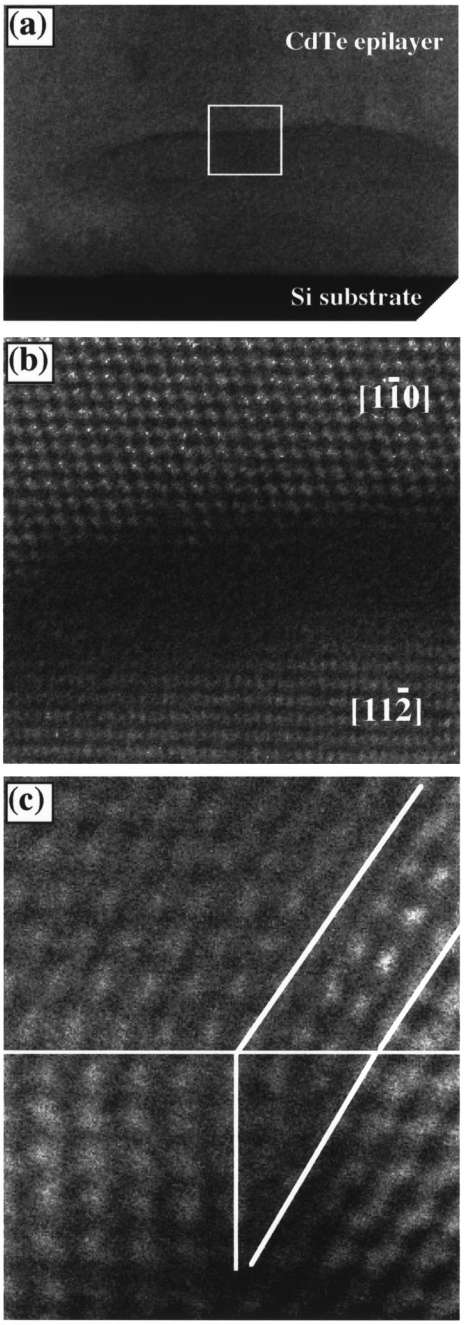

FIG. 7. (a) Low magnification annular dark field STEM image looking down [1−10]CdTe/[110]Si, showing an overgrown small grain in a thick film. (b) Enlargement of the boxed region in (a) showing the small 90° rotated domain down [11−2] with the main matrix down [1−10]. (c) Another high-resolution *Z*-contrast image of the CdTe layer down [1−10] showing the merging of 180° rotated domain by twinning.

brighter on the upper row of the CdTe double layer. This is comfirmed by the intensity profile. Therefore, clearly the polarity is (111)B. We note that the polarity of the thick film was determined from bulk regions of the film, well away from the CdTe/Si interface area which contains both (111)B and (111)A domains.

CBED is also used to confirm the *Z*-contrast result, although in this case a reference sample must be used. There has been much confusion over the years concerning the polarity determined by electron diffraction, perhaps because of the rotation of the image relative to the diffraction pattern introduced by electron microscope or the 180° ambiguity during computer simulation. This is overcome here by using a reference sample [a (111)B GaAs],[21] whose polarity is known absolutely. There are several different ways of using CBED or microdiffraction to determine the polarity.[22–24] Here a [1−10]CdTe zone axis CBED pattern is taken from a perfect region close to the growth surface of the film, shown in Fig. 9(a). Comparing with the simulations [Fig. 9(b)] using EMS software,[25] {111}B and {111}A disks are distinguished and assigned. It is worth mentioning that Debye–Waller factors are very important in the CdTe CBED simulations and they must be included in the calculations to get comparable results to the experimental data. By comparing to the reference sample to get the right image rotation, it is confirmed that the thick film has a (111)B polarity. Chemical etching using 1:1:1 HF:HNO_3:acetic acid (or lactic acid) turns the (111)A polar surface matt black, while leaving the (111)B surface shiny.[23,26] Our etching results also confirm

Downloaded 04 Jun 2004 to 160.91.48.238. Redistribution subject to AIP license or copyright, see http://jap.aip.org/jap/copyright.jsp

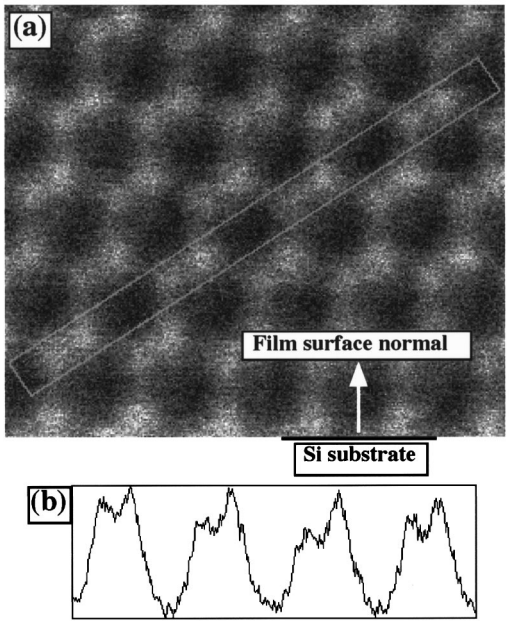

FIG. 8. High-resolution *Z*-contrast image down [1−10]CdTe taken from a region close to the growth surface of the thick film. The individual Cd and Te atomic columns are clearly shown, indicating a Te-terminated film. (b) Profile of the boxed region in (a).

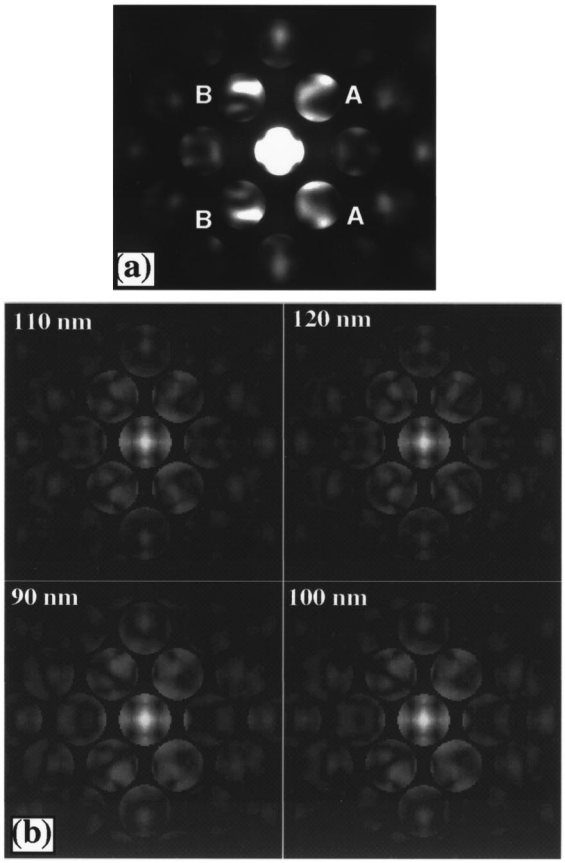

FIG. 9. (a) [1−10] convergent beam diffraction pattern taken from the region close to the growth surface of the thick film. {111}B and {111}A diffraction discs are indicated as B and A, respectively. (b) Simulations of the experimental CBED pattern in (a) with different film thickness.

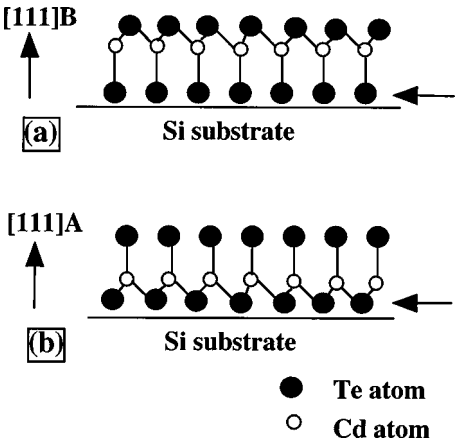

FIG. 10. Sketches showing the formation of domains with different polarities at the interface. (a) (111) B domain is formed when the first Te layer has one upward bond to form with Cd atoms; (b) (111)A domain is formed when the first Te layer has three upward bonds to form with Cd atoms;

that the polarity of the thick film is (111)B CdTe. The results from all three different techniques are consistent, and demonstrate that the polarity of the final CdTe thick film grown on the (001)Si substrate is (111)B, confirming previous results.[8,20]

IV. DISCUSSION OF THE GROWTH MECHANISM

The comprehensive view of the microstructure of the films described above allows us to significantly extend existing models for the growth of CdTe on Si.[8,9,10,27,28] In the initial stage of film growth, Te atoms are deposited first and either bond to or substitute Si surface atoms.[8,27,29,30] The polarity of each domain is determined by the bonding of the first Te layer in the film. If there is one active bond to form with Cd, then the polarity will be (111)B and if there are three active bonds, the domain will have (111)A polarity (as shown in Fig. 10). Our present observations show that in fact the majority domains nucleated with a (111)B polarity, with few having the opposite (111)A polarity in this initial phase of film growth. The pretreatment of the substrate surface using a Te flux before growth and the annealing at the initial stage may enhance the possibility for Te atoms to have one active bond, which gives rise to the preferential growth of domains with (111)B polarity. Work is currently underway to investigate the interface between (111)B domain and Si substrate by high-resolution *Z*-contrast imaging. However, in this article we will concentrate the discussion on the evolution of the final film morphology after the nucleation stage.

On a nominal (001)Si substrate surface, which has fourfold symmetry due to the paired S_B and S_A terraces, there are eight possible orientations for a CdTe domain, four rotational variants, each with two polarities, as shown in Fig. 11. These are (111)A or (111)B domains, 180° rotated domains with [11−2]CdTe aligned with either [110]Si or [−1−10]Si, or 90° rotated domains with [11−2]CdTe along either [110]Si or [1−10]Si With no optimized growth conditions, these variants would result in multidomain films. However, by using optimized growth conditions, the pretreatment of the substrate surface using a Te flux and a miscut Si substrate, the

Downloaded 04 Jun 2004 to 160.91.48.238. Redistribution subject to AIP license or copyright, see http://jap.aip.org/jap/copyright.jsp

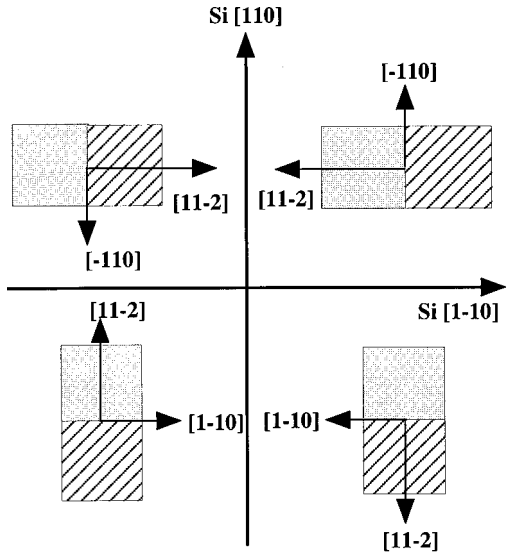

FIG. 11. Sketch showing a top view of a nominal (001)Si with eight types of domains. The different shaded area denote different polarities, i.e., (111)A and (111)B.

symmetry is broken and it is very reasonable that one type of domain will dominate, as we have found. The (111)B type domains with orientation of [11−2]CdTe//[1−10]Si are found to be larger in size, and connected with each other. The formation of this dominating domain could occur in the following way.

When the Si substrate is miscut, tilting by (θ, ϕ) away from [001], the symmetries along the [1−10] and [−110] directions are broken, with wider S_B terraces and narrower S_A terraces along [110], and kinks also run along [1−10] of the step edges in a preferential direction.[9,10,28] In such situations, it is clearly likely that the formation of CdTe nuclei of different types will have different probabilities, as shown in Fig. 12. The kinks at the step edges may guide the CdTe nuclei into a preferred orientation out of the two 180° rotations. The wider S_B terraces combined with low mismatch along the step edge on these terraces may enhance the growth and spread of the domains [11−2]CdTe//[1−10]Si

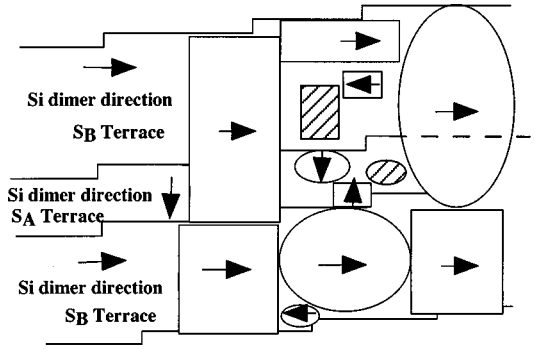

FIG. 12. Diagram schematically showing a top view of the nucleation of different domains on a miscut (001)Si substrate. The grains of the dominating domain are denoted with larger size. The arrows represent the direction of [11−2]CdTe. The shaded area indicates minority grains with (111)A polarity.

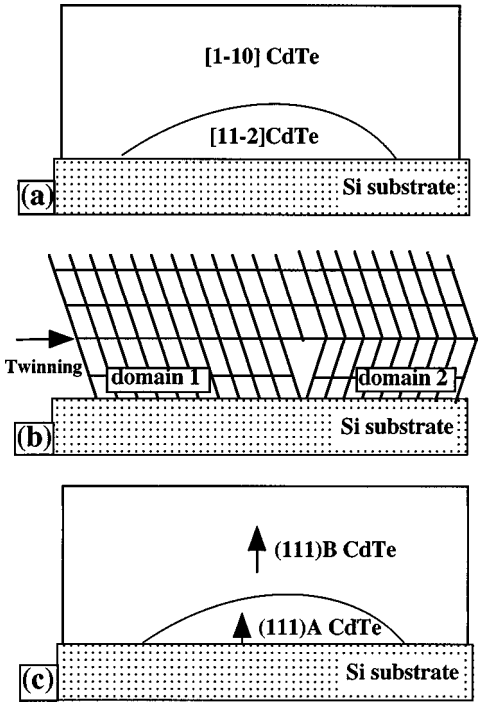

FIG. 13. Sketches of a cross-sectional view of the thick film showing the overgrown mechanisms. (a) The dominating domain overgrows the smaller 90° rotated domain; (b) merging into one domain by twinning; (c) (111)B domain overgrows (111)A due to growth kinetics.

over the 90° rotated domains on the S_A terraces. This breaking of the initial surface symmetry is an important element in the growth process, because it allows the possibility of one domain dominating over the other minority domains. In the sample observed here, the dominating domain has (111)B polarity with an orientation of [11-2]CdTe along [1−10]Si on the wider S_B terraces.

As growth proceeds, the CdTe islands coalesce through the reactions we have presented above, which are depicted schematically in Fig. 13. Due to the dominating domains prevailing on the substrate and energetically favorable, they tend to grow faster not only laterally, but also vertically, and finally overgrow the minority 90° rotated domains [Fig. 13(a)]. For the 180° rotated domains, twinning on the (111) plane in one grain would then lead to a single domain [Fig. 13(b)]. The faster growth of (111)B domains could easily overgrow the (111)A polarity domains due to growth kinetics alone [Fig. 13(c)]. Through these reactions, the final film has its single-crystal character. The final film orientation is obtained as a result of competing growth kinetics.

V. CONCLUSIONS

In summary, a comprehensive picture of the growth and microstructure of (111)B CdTe films grown on (001)Si substrate has been developed by a combination of several TEM techniques and high-resolution *Z*-contrast imaging on a STEM. Experimental data shows that the initial stage of growth, the CdTe nucleates with different types of domains, although the dominant domain is (111)B polarity with [11−2]CdTe parallel to [1−10]Si. Planar defects, such as microtwins and stacking faults grow on both (111)B and

Downloaded 04 Jun 2004 to 160.91.48.238. Redistribution subject to AIP license or copyright, see http://jap.aip.org/jap/copyright.jsp

(111)A planes during the nucleation stage. The final polarity of the thick film is (111)B as determined by CBED, high-resolution *Z*-contrast imaging, and chemical etching. Breaking the substrate symmetry through a specific miscut not only creates a large number of steps to assist in the nucleation of CdTe islands, but also induces one domain orientation to dominate. As growth proceeds, a single-crystal film forms as the dominating domain overgrows the minority domains. This is the fast growing (111)B domain with [11−2]CdTe parallel to [1−10]Si, which through various growth processes overgrows the other orientations to result in the single-crystal film.

ACKNOWLEDGMENTS

This research was sponsored by DOE under Grant No. DOE DE-GF02-96ER45610 with University of Illinois at Chicago and Contract No. DE-AC05-96OR22464 with Lockheed Martin Energy Research Corporation. The Advanced Research Projects Agency is acknowledged for its support under AFOSR Contract No. F49620-94-C-0080. Dr. K. B. Alexander of Metal and Ceramic Division, Oak Ridge National Laboratory is acknowledged for the permission to use Philips CM 12 and Philips CM30 microscopes. Dr. P. D. Brown from Cambridge University of U.K. is acknowledged for the provision of reference sample and helpful discussions, and Dr. K. Durose from Durham University of U.K., Dr. C. H. Grein, from University of Illinois at Chicago, and Dr. H. Tatsuoka from Shizuoka University of Japan are thanked for helpful discussions.

[1] H. Ebe, T. Okamoto, H. Nishino, T. Saito, Y. Nishijima, M. Uchikoshi, M. Nagashima, and H. Wada, J. Electron. Mater. **25**, 1358 (1996).
[2] I. Bhat and W. S. Wang, Appl. Phys. Lett. **64**, 566 (1994).
[3] H. Nishino and Y. Nishijima, J. Cryst. Growth **167**, 488 (1996).
[4] R. Korenstein, P. Madison, and P. Hallock, J. Vac. Sci. Technol. B **10**, 1370 (1992).
[5] H. Tatsuoka, H. Kuwabara, Y. Nakanishi, and H. Fujiyasu, J. Cryst. Growth **129**, 686 (1993).
[6] R. Sporken, S. Sivananthan, K. K. Mahavadi, G. Monfroy, M. Boukerche, and J. P. Faurie, Appl. Phys. Lett. **55**, 1879 (1989).
[7] R. Sporken, M. D. Lange, C. Masset, and J. P. Faurie, Appl. Phys. Lett. **57**, 1449 (1990).
[8] R. Sporken, Y. P. Chen, S. Sivananthan, M. D. Lange, and J. P. Faurie, J. Vac. Sci. Technol. B **10**, 1405 (1992).
[9] Y. P. Chen, S. Sivananthan, and J. P. Faurie, J. Electron. Mater. **22**, 951 (1993).
[10] Y. P. Chen, J. P. Faurie, S. Sivananthan, G. C. Hua, and N. Otsuka, J. Electron. Mater. **24**, 475 (1995).
[11] L. A. Almeida, Y. P. Chen, J. P. Faurie, S. Sivananthan, D. J. Smith, and S.-C. Y. Tsen, J. Electron. Mater. **25**, 1402 (1996).
[12] I. Sugiyama and Y. Nishijima, Appl. Phys. Lett. **66**, 2798 (1995).
[13] Unpublished results.
[14] J. T. Cheung, Appl. Phys. Lett. **51**, 1940 (1987).
[15] S. Sivananthan, X. Chu, J. Reno, and J. P. Faurie, J. Appl. Phys. **60**, 1359 (1986).
[16] M. Kawano, N. Oda, T. Sasaki, T. Ichihashi, S. Iijima, T. Kanno, and M. Saga, J. Cryst. Growth **117**, 171 (1992).
[17] P. D. Brown, Y. Y. Loginov, W. M. Stobbs, and C. J. Humphreys, Philos. Mag. A **72**, 39 (1995).
[18] R. J. Koestner and H. F. Schaake, J. Vac. Sci. Technol. A **6**, 2834 (1988).
[19] E. P. Warekois, M. C. Lavine, A. N. Mariano, and H. C. Gatos, J. Appl. Phys. **33**, 690 (1961).
[20] C. Hsu, S. Sivananthan, X. Chu, and J. P. Faurie, Appl. Phys. Lett. **48**, 908 (1986).
[21] P. D. Brown (private communication).
[22] P. Spellward and A. R. Preston, Inst. Phys. Conf. Ser. **93**, 29 (1988).
[23] E. A. Hewat, L. DiCioccio, A. Million, M. Dupuy, and J. P. Gailliard, J. Appl. Phys. **63**, 4929 (1988).
[24] P. D. Brown, K. Durose, G. J. Russell, and J. Woods, J. Cryst. Growth **101**, 211 (1990).
[25] P. A. Stadlelamn, Ultramicroscopy **21**, 131 (1987).
[26] K. Durose (private communication).
[27] D. J. Wallis, N. D. Browning, S. Sivananthan, P. D. Nellist, and S. J. Pennycook, Appl. Phys. Lett. **70**, 3113 (1997).
[28] J. Oh and C. H. Grein, J. Cryst. Growth **179**, 72 (1997).
[29] M. R. Bennett, A. A. Cafolla, J. W. Cairns, C. J. Dunscombe, and R. H. Williams, Surf. Sci. **360**, 187 (1996).
[30] S. R. Burgess, B. C. C. Cowie, S. P. Wilks, P. R. Dunstan, C. J. Dunscombe, and R. H. Williams, Appl. Surf. Sci. **104**, 152 (1996).

Downloaded 04 Jun 2004 to 160.91.48.238. Redistribution subject to AIP license or copyright, see http://jap.aip.org/jap/copyright.jsp